Real-Time Detection and Localization of Line Trip Event via Relative Phase Angles

He Yin, *Senior Member, IEEE*, Wei Qiu, *Member, IEEE*, Yuru Wu, *Student Member, IEEE*, Shutang You, *Senior Member, IEEE*, Yuqing Dong, *Member, IEEE*, Wenpeng Yu, *Member, IEEE*, and Yilu Liu, *Fellow, IEEE*

***Abstract*—Line trip events widely exist in power systems. They can result in power outages and a huge economic loss if not promptly detected and localized. To provide a fast and precise solution, this article presents a Complete Coverage of Voltage Measurement (CCVM)-based line trip event detection algorithm and a Relative Phase Angle (RPA)-based line trip event localization algorithm. First, frequency and relative phase angle features during a line trip event are calculated. Then, the CCVM-based algorithm is proposed from both frequency and rate of change of frequency estimation algorithm aspects. Additionally, the RPA-based algorithm is presented, and two cases are studied to demonstrate the uniqueness of the proposed algorithm. Various experiments are conducted, where the simulation results demonstrate that the proposed CCVM-based algorithm can detect a line trip event as short as 2.07 ms. In addition, the RPA-based algorithm has 1.26 times higher localization accuracy compared with the frequency magnitude-based and phase angle-based algorithms. The experiment results on the examples from two interconnected power systems in the U.S. verified the performance of the proposed algorithms in wide-area power systems.**

***Index Terms*—Line trip event detection, event localization, relative phase angle, wide-area power systems.**

I. Introduction

EVENT detection and localization in power systems are of great importance to both utility companies and federal governments for prompt responses and preparations [1]. With the increasing number of Distributed Energy Resources (DERs) integrating into power systems, the disturbances caused by DERs are becoming one of the major sources of events [2], [3]. Among power system events, line trips are one of the common events which can be caused by either line outage or line maintenance. Therefore, the fast line trip event detection and precise localization are valuable to event elimination.

Normally, the line trip event detection and localization algorithms can be categorized into model-based and data-based algorithms. In [4], the authors use a power-flow model and statistical-change-detection theory with limited measurements to detect the line trip event. Similarly, a new Alternating Current (AC) power-flow model is proposed to estimate the location of the line trip event in [5]. A load-stochastic-perturbation-based multiple line trip event detection algorithm is presented in [6]. [7] introduced a graph-spectral-analysis-based line trip event detection and localization algorithm through leveraging the power grid topology. However, the primary drawback of the model-based algorithms is the scalability. It is challenging to apply the model-based algorithms to a new power system without detailed models.

Conversely, data-based algorithms can be more model friendly. One of the most common data sources is the Supervisory Control and Data Acquisition (SCADA) system in the operation center [8]. It can simply detect line trip events by checking the status of breakers with low computational burden and lower transmission information. Although the SCADA system is able to localize line trips from protection relies on, it lacks the big picture of the entire power system since there are several power utilities in a wide area, e.g., the U.S. power grid, and they can only get access to their own SCADA system. In addition, the delay of the SCADA is a barrier to the fast and precise line trip event detection and localization. In contrast, using synchronized measurements from Phasor Measurement Units (PMUs) as the data source have unique advantages such as accurate measurements and fast response capabilities [9]. Moreover, if a current-based PMU is deployed at one end of the tripped line, it can be straightforward to detect and localize the line trip event by checking with the current magnitudes. Additionally, the utility companies can be informed in real-time and the federal governments can take prompt responses to avoid huge economic loss from the events based on the online detection results.

The existing PMU-based line trip event detection and localization algorithms are mainly utilizing phase angle and frequency measurements from both current and voltage waveforms. The

Manuscript received 24 October 2022; revised 4 April 2023; accepted 12 June 2023. Date of publication 19 June 2023; date of current version 21 February 2024. This work was supported in part by Engineering Research Center shared facilities, in part by Engineering Research Center Program of the National Science Foundation (NSF), in part by the Department of Energy under NSF Award Number EEC-1041877, and in part by the CURENT Industry Partnership Program. Paper no. TPWRS-01613-2022. *(Corresponding author: Wei Qiu.)*

He Yin, Wei Qiu, Yuru Wu, Shutang You, Yuqing Dong, and Wenpeng Yu are with the Department of Electrical Engineering and Computer Science, The University of Tennessee, Knoxville, TN 37996 USA (e-mail: hyin8@utk.edu; qwei4@utk.edu; ywu70@vols.utk.edu; syou3@utk.edu; ydong22@utk.edu; wyu10@utk.edu).

Yilu Liu is with the Department of Electrical Engineering and Computer Science, The University of Tennessee, Knoxville, TN 37996 USA, and also with the Oak Ridge National Laboratory, Oak Ridge, TN 37831 USA (e-mail: Liu@utk.edu).

Color versions of one or more figures in this article are available at https://doi.org/10.1109/TPWRS.2023.3287233.

Digital Object Identifier 10.1109/TPWRS.2023.3287233

0885-8950 © 2023 IEEE. Personal use is permitted, but republication/redistribution requires IEEE permission.
See https://www.ieee.org/publications/rights/index.html for more information.

Authorized licensed use limited to: UNIVERSITY OF TENNESSEE LIBRARIES. Downloaded on April 18,2024 at 21:44:51 UTC from IEEE Xplore. Restrictions apply.

line trip event will cause the active power flow step to change on both sides of the tripped line so that phase angles will change based on the active power values. Based on this idea, [10] proposed line trip event detection using phasor angle measurements. However, this method does not have the ability to localize the event. Additionally, a quick-change detection algorithm targeting searching the largest phase angle variation is proposed in [11]. Since the phase angle variation is proportional to the frequency value, it would be equal to checking the frequency measurements. By checking the frequency spike, a line trip event can be promptly detected [12]. The frequency spikes during the line trip event can be an obvious feature to identify. However, this is not commonly true for all circuit cases where the frequency spikes on the ends of the tripped line are in opposite directions and magnitude values can be smaller than those on other buses. This could mislead the line trip event localization and reduce the accuracy.

The active power flow is another variable that can be calculated to localize the line trip event if both voltage and current measurements are available [13]. The voltage and current synchrophasors collected from the PMUs are also used to identify the fault location [14], [15]. The [16] treats the generation trip event location estimation as a nonlinear optimization problem. The dynamic state estimation and gradient descent are also used to localize the transmission line fault [17]. Besides, to precisely identify the location of the line trip, conventional machine learning methods are used, including the support vector machine [18], and K-means clustering [19]. For example, the effectiveness of the K-means clustering is verified by using the simulation cases within 2 seconds [19]. Taking advantage of the high precision of artificial intelligence, such as long short-term memory networks [20], the artificial intelligence methods are also utilized to detect the event. For example, [21] and [22] developed the convolutional autoencoders and ensemble model to achieve anomaly detection. By estimating the state of the event, a dynamic programming based on swinging door trending is proposed in [23] to accurately detect the start time of an event and the event placement so that the fault events can be instantly cleared. However, a large number of training event samples is required, and its robustness will decrease if the parameters of the model cannot be universal.

Taking advantage of the high precision of artificial intelligence, such as long short-term memory networks [20], the artificial intelligence methods are also utilized to detect the event. However, a large number of training event samples is required, and its robustness will decrease if the parameters of the model cannot be universal.

Frequency Monitoring Network (FNET) is one of the wide-area measurement systems (WAMSs) that provide fast and precise monitoring of power systems by using PMU measurements [24]. Operating by the University of Tennessee, Knoxville and Oak Ridge National Laboratory (ORNL), FNET is currently targeting on the power system situational awareness from a national-wide power system point of view [25]. One of the major functions of the FNET is to detect and localize the line trip event by using the real-time measurements steamed from PMUs.

In this article, a line trip event detection algorithm together with a localization algorithm are proposed and deployed in the FNET. The major contributions can be summarized as follows:

- A novel Complete Coverage of Voltage Measurement (CCVM)-based algorithm is designed from both frequency and Rate of Change of Frequency (RoCoF) estimation algorithm aspects to avoid missing the line trip events. This algorithm can also detect the line trip event at a fast speed by using high-speed measurements.
- To precisely localize the line trip event, a Relative Phase Angle (RPA)-based algorithm is proposed considering both power flow direction change and fewer sensor cases, where the real-time RPA measurements are used. This algorithm can localize line trip events in a wide area.
- The tests based on the IEEE 9 and 39 bus standard systems [26] are carried out. Importantly, by deploying the proposed method in FNET, the actual field test data from both U.S. Eastern Interconnection (EI) and Western Electricity Coordinating Council (WECC) systems are collected and tested. Experimental results demonstrate that the proposed CCVM-RPA can achieve the real-time event localization even under power flow direction change and limited number of sensor cases.

II. Model of Line Trip Events

Line trip events can be caused by the outage that happened on transmission lines as a result of the bad weather or accidents. It can also be caused by power system operations, such as breaker and switch operations for maintenance purposes. To successfully detect and localize the line trip event, the relative phase angle-based numerical model is established.

A typical line trip event is illustrated in Fig. 1. Assuming a line trip event happens between Bus 0 and 1, the line trip event will directly cause the power flow through this line to become zero which can be treated as two active power injections (marked as red current sources) to the buses adjacent to the tripped line with opposite directions onto the original power flow. The power flow variations will further lead to phase angle variations so that a frequency spike will be observed because the frequency is the derivative of the phase angles. The relationship among the active power, the voltage magnitude, and the voltage phase angle is given as,

$$P_{i,j} = \frac{|V_i||V_j|}{|X_{i,j}|}\sin(A_{i,j}), \tag{1}$$

where $P_{i,j}$ is the active power flow sending from bus i to bus j, V_i and V_j are the bus voltages on the bus i and j, $X_{i,j}$ is the line impedance between bus i and j, and $A_{i,j}$ is the phase angle difference between bus i and j which is usually less than $\pi/2$.

Based on (1), once a power step change happens, the $A_{i,j}$ will have a step change as well assuming the V_i and V_j are constant because of their relatively small changes during line trip events. Notice that voltage magnitude can also be utilized for event detection in small-scale power grids, e.g., microgrids [27].

To further study the $A_{i,j}$ in other lines adjacent to the tripped line, an illustration for the line outage is given in Fig. 1 to show

Authorized licensed use limited to: UNIVERSITY OF TENNESSEE LIBRARIES. Downloaded on April 18,2024 at 21:44:51 UTC from IEEE Xplore. Restrictions apply.

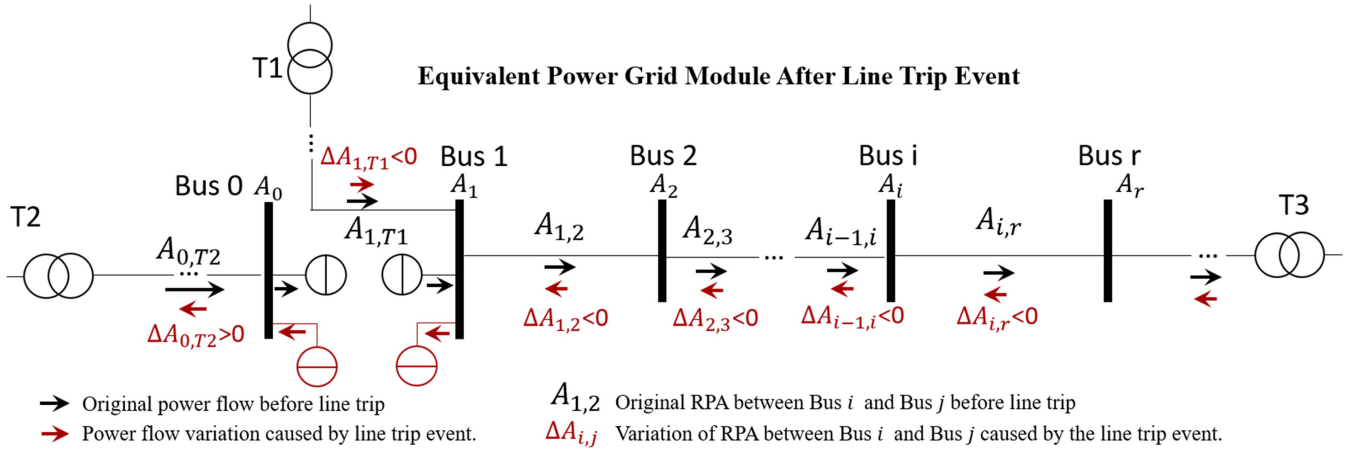

Fig. 1. Illustration of the line trip event.

the power flows and relative phase angles in the following lines. A multiple bus system with three transformers is given with power flow marked in black arrow. After the line trip event happened, the power flow variations caused by the line trip event are also marked as red arrow. Note that the power flow directions may changed after line trip events but the power flow variation direction can be determined by the grid topology and event location. The RPA variation between bus i and bus r can be written as,

$$A_{i,r} = A_i - A_r = \sum_{j=i}^{r-1} A_{j,j+1}, \tag{2}$$

$$= \sum_{j=i}^{r-1} A'_{j,j+1} + \sum_{j=i}^{r-1} \Delta A_{j,j+1}, \tag{3}$$

$$\Delta A_{i,r} = A_{i,r} - A'_{i,r} \tag{4}$$

$$= \sum_{j=i}^{r-1} \Delta A_{j,j+1} \tag{5}$$

where $A_{i,r}$ is the RPA between bus i and bus r after the line trip event, $A'_{i,r}$ is the RPA between bus i and bus r before the line trip event, and $\Delta A_{i,r}$ is the RPA variation between bus i and bus r before and after the event. A_i and A_r are the voltage phase angle before the line trip event in bus i and bus r, respectively. Since the two injected active power injections are in opposite directions, the sign of the $\Delta A_{0,T2}$ and $\Delta A_{i-1,i}$ $(i = 1, 2, \ldots, T3)$ can be written as,

$$\Delta P_{0,T2} > 0 \Rightarrow \Delta A_{0,T2} > 0, \tag{6}$$

$$\Delta P_{i-1,i} < 0 \Rightarrow \Delta A_{i-1,i} < 0,$$
$$i = 1, 2, \ldots, T_3, \tag{7}$$

where $\Delta P_{0,T_2}$ and $\Delta A_{0,T2}$ are the power flow and RPA variations from bus $T2$ to bus 0, $\Delta P_{i-1,i}$ and $\Delta A_{i-1,i}$ are the power flow and RPA variation from bus $i-1$ to bus i. Based on (5), the $\Delta A_{i-1,r}$ can be written as,

$$\Delta A_{i-1,r} = \Delta A_{i-1,i} + \Delta A_{i,r} < \Delta A_{i,r}, \tag{8}$$

TABLE I
FREQUENCY ALGORITHM WINDOW SIZE OPTIONS

Minimum reporting rate(Hz/s)	10	12	15	20	30	60
Window size (cycle)	6	5	4	3	2	1

$$\Delta A_{1,r} < \Delta A_{2,r} < \ldots < \Delta A_{i,r} < 0. \tag{9}$$

Based on (9), the RPA variation decreases from the tripped line location to the end of this line. It is the same as the other side of the tripped line but the RPA variation direction is in the opposite way.

III. Line Trip Event Detection Algorithm

A. Improved Frequency and RoCoF Estimation

As discussed in Section II, frequency spikes will be observed during a line trip event because of the phase angle step change. Since frequency spikes can be directly captured by checking with the RoCoF values, the frequency estimation algorithm is essential for line trip event detection. There are many existing frequency estimation algorithms where classical ones are zero-crossing [28], phase lock loop (PLL) [29], and discrete Fourier transform (DFT)-based algorithms.

Usually, DFT-based algorithms use a relatively longer data window to cover the complete voltage waveform [30]. The relationship among reporting rate and the window size, and nominal frequency is calculated as,

$$f_0 = W_{DFT} * T_R, \tag{10}$$

where f_0 is the nominal frequency, W_{DFT} is the DFT window size and T_R is the reporting rate.

The detailed relationship between the minimum reporting rate and DFT window size is summarized in Table I. Based on the IEEE C37.118.1 [31], the frequency reporting rate ranges from 10 to 60 Hz. Therefore, the W_{DFT} should be designed from 6 to 1 cycle accordingly, as shown in Fig. 2. The above results reveal that a 1-cycle-based DFT is sensitive compared with a 6-cycle-based DFT. And for a PMU with a higher reporting rate,

Authorized licensed use limited to: UNIVERSITY OF TENNESSEE LIBRARIES. Downloaded on April 18,2024 at 21:44:51 UTC from IEEE Xplore. Restrictions apply.

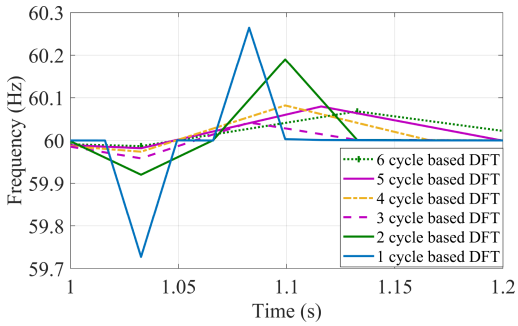

Fig. 2. Frequency estimation algorithm among different window sizes.

a short window is the optimal solution considering the resolution of the high RoCoF values during the line trip event. Note that this frequency estimation algorithm is only utilized for line trip event detection purposes so the static state measurement accuracy may be not good enough compared to the algorithm using a short DFT window. To detect line trip events rapidly, a high-speed frequency estimation algorithm with 1440 Hz reporting rate and 1 cycle DFT window size (with three frequency measurements) is utilized.

The RoCoF can directly detect the frequency spikes by threshold-based algorithms. Since the target for this RoCoF estimation is to capture the frequency spikes, which have the features of low-frequency duration and large frequency magnitude change, the RoCoF can be calculated by utilizing a curve-fitting algorithm with a short window [32].

Besides, the local RoCoF is closely related to the local inertia and local event power [33]. Their relationship can be described as $P_{event} = 2I/f_N$ RoCoF, where I is the local inertia, f_N is the nominal frequency, and P_{event} is the local power imbalance. Although the RoCof is impacted by inertia, the power imbalance will dominate the RoCof when it is not too far from the event location. Thus, the RoCoF of the buses near the line-trip event will be much larger, assuming the inertia is not changing fast in one line.

Based on (7), we can assume $\Delta A_{i-1,i} = 0$, $f_{i-1} = f_i$, and $RoCoF_{(i-1)} = RoCoF_i$ at $t = 0$. For $t = dt$, considering the frequency is the derivate of phase angle. For $t = dt$, it can be inferred that

$$\Delta A_{i-1} < \Delta A_i \rightarrow f_{i-1} < f_i \rightarrow \mathrm{RoCoF}_{i-1} < RoCoF_i \quad (11)$$

Since $RoCoF_{(i-1)} < 0$ and $RoCoF_i < 0$, we got:

$$|\mathrm{RoCoF}_{i-1}| > |\mathrm{RoCoF}_i| . \quad (12)$$

It can be derived that the RoCoF of the buses near the line-trip event will be larger than remote buses, therefore RoCoF can be only suitable for identifying the PMU near-the-line trip event.

B. CCVM-Based Line Trip Event Detection Algorithm

Based on the frequency and RoCoF estimation algorithms, a CCVM-based line trip event detection algorithm is proposed in Fig. 3. The detection of the line trip contains two stages.

CCVM line trip event detection: The first stage is to calculate the RoCoFs, and then compare them with threshold T_m. If the absolute value of the RoCoF is higher than T_m which means the first half of the frequency spike is detected, the next j RoCoFs will be saved. A 2 s window is selected which means 2880 RoCoFs is calculated. Then, the frequency peak will be checked by the sign of $RoCoF(i)RoCoF(j)$ to filter all the PMUc (PMUs that are close to the line trip event). Note that the frequency spike may have two directions so that absolute values are taken for the threshold comparison.

The improvements of the CCVM-based algorithm are 1) the entire waveform is scanned by choosing the appropriate frequency estimation algorithm and reporting rate; 2) the line trip event detection is very sensitive since a 1 cycle-based DFT algorithm is used; 3) the detection time can be as short as 2.07 ms since the sliding window with step 3 is selected under the 1440 Hz reporting rate. This can be helpful for the operators of utility companies to confirm the event and have a prompt response accordingly.

Here, the T_m depends on the frequency estimation algorithm, the rated active power flow of the transmission line, and the impacted PMU number. It is designed as a user-defined value to tune the sensitivity of the line trip event detection algorithm since the RoCoF of the line trip event is much higher than the RoCoF from other events [34]. In order to distinguish the line trip events from other events, such as inverter-based resource injection, generation trip, short circuit faults, and power swings, an event RoCoF statistical analysis is required. For example, the T_m is set to 0.005 Hz/s in this research based FNET/GridEye historical data and the event library.

There are limitations to the CCVM-based algorithm such as failure to distinguish the line trip events from breaker operations and load-switching events. This is because these events contain frequency spikes in their frequency responses that will trigger the frequency spike detection.

IV. Line Trip Event Localization Algorithm

A. RPA-Based Algorithm

Before starting the localization, the system topology is required which is assumed to be known in this article. The system topology can be accessed through the breaker statuses from SCADA or estimated by some measurement-driven algorithms, e.g., [35]. It would be straightforward to use the frequency magnitude value to identify the line trip event location. However, this is not accurate if the impedance of the lines varies too much. As discussed in Section II, RPAs close to the line trip event location have larger values.

To increase the location accuracy, the RPA-based line trip event localization algorithm is proposed.

Line trip localization: The first step of the RPA-based algorithm is to identify the PMU deployment information so that the PMUc can be utilized for line trip events localization purposes. Then calculate the relative phase angles to judge the power flow direction. By corporating the topology reconfiguration -based algorithm, a limited number of PMU cases would be proposed to find the candidate buses and lines.

Authorized licensed use limited to: UNIVERSITY OF TENNESSEE LIBRARIES. Downloaded on April 18,2024 at 21:44:51 UTC from IEEE Xplore. Restrictions apply.

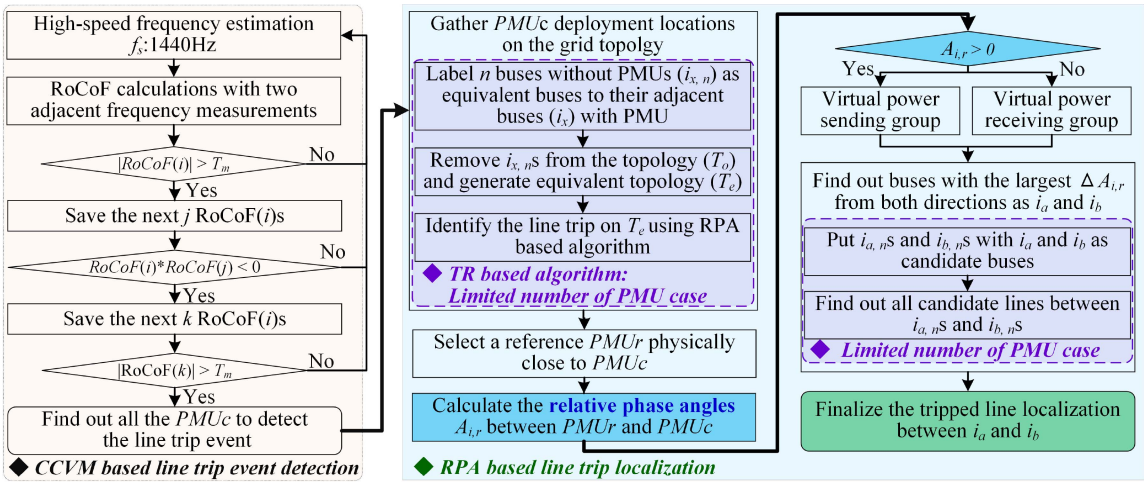

Fig. 3. Illustration of the flowchart for the entire algorithm from detection to localization.

Denoted the PMU_c as the PMU that close to the line trip event, as illustrated in Fig. 3, the first step of the RPA-based algorithm is to identify the PMU deployment information so that the PMU_cs can be utilized for line trip events localization purposes. To calculate the relative phase angles, a reference PMU_r with a lower $|RoCoF|$ will be selected physically close to PMU_cs. Then, by subtracting the phase angles from PMU_cs and PMU_r, the relative phase angles, $A_{i,r}$ can be calculated easily as below,

$$A_{i,r} = A_i - A_r. \tag{13}$$

Through checking the $A_{i,r}$ after line trip event, PMU_cs can be categorized into Virtual Power Sending Group (VPSG) and Virtual Power Receiving Group (VPRG) depending on the sign of RPAs. Note that the VPSG and VPRG may not reflect the true power flow direction depending on the reference PMU selection.

The next step is to pick out the largest RPAs from both positive and negative directions so that the buses with the largest $\Delta A_{i,r}$ can be found as,

$$i_a = \text{find}[\Delta A_{i,r} = \max(\Delta A_{i,r})], \tag{14}$$

$$i_b = \text{find}[\Delta A_{i,r} = \min(\Delta A_{i,r})], \tag{15}$$

where i_a and i_b are the two buses with the largest $\Delta A_{i,r}$ in two opposite directions. Finally, all connected lines between i_a and i_b are treated as the candidate tripped line locations.

B. Power Flow Direction Change Case

There is a special case where the line trip event will change the power flow direction of one end bus if there are no other alternative lines to support the load power. In this case, both $A_{i,r}$s on two ends of the tripped line will have large oscillations so that both maximum and minimum frequency drop will be on one end bus and other adjacent buses. In order to identify the line trip event under this special case, the buses with the largest two $A_{i,r}$ oscillation magnitudes are utilized as the candidate end bus.

For a line trip case in the radial circuit, the outage may happen, which means that event can be detected from the PMUs that were shunted down.

C. Limited Number of Sensor Case

In real-world cases, there may not have PMUs deployed on all buses. The regular maintenance and the cost of installation have also limited PMU deployments. However, the minimum number of PMUs to identify the line trip location remains an issue since it highly depends on the system topology and line trip locations. In this article, an alternative method to estimate the line trip location by listing all candidate buses is presented.

In this regard, a Topology Reconfiguration (TR)-based algorithm is proposed to modify the RPA-based algorithm with fewer sensor cases. The basic idea is to combine n buses without PMU ($i_{x,n}$) to an adjacent bus with PMU (i_x). The detailed algorithm flow chart is illustrated in Fig. 3. The first step is to label $i_{x,n}$s as equivalent buses to i_xs.

In this case, an equivalent bus (i'_x) can be utilized to represent the multiple buses ($i_{x,n}$s and i_x). Then, the $i_{x,n}$s will be removed from the topology (T_o) so that the less sensor case becomes a full sensor case in the equivalent topology (T_e). Thus, the line trip event can be easily identified through the RPA-based algorithm. Meanwhile, the $i_{a,n}$s and $i_{b,n}$ should also be listed as the candidate end buses of the tripped line together with i_a and i_b given in (14) and (15). Finally, all possible lines between two candidate bus groups will be treated as the candidate tripped lines based on the grid topology. Instead of precisely identifying the tripped line, this algorithm provides a group of candidate tripped lines if PMU deployment is insufficient to identify the tripped line precisely.

D. Islanded System Case

The line trip event may cause the power system separation and thus lead to an islanded system. As shown in Fig. 3, the proposed line trip event detection and localization algorithms will only use 2 s measurements right after the line trip event happened. Thus,

Authorized licensed use limited to: UNIVERSITY OF TENNESSEE LIBRARIES. Downloaded on April 18,2024 at 21:44:51 UTC from IEEE Xplore. Restrictions apply.

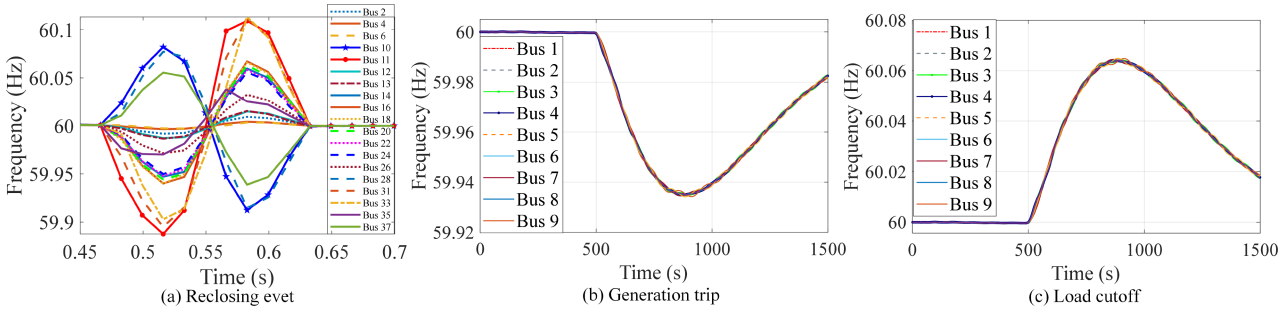

Fig. 4. Frequency responses of example events. (a) Reclosing event. (b) Generation trip. (c) Load cutoff.

the phase angles inside and outside of the islanded system are still synchronized. The proposed algorithms can still work under islanded system case.

However, the phase angles inside and outside of the islanded system will become synchronized after a period of time. As shown in Fig. 3, the proposed algorithm will be combined with the islanding detection algorithm proposed in [36]. Multiple detection and localization algorithms will run in parallel for each islanded system.

E. Reclosing Case

Due to the protection system in the breakers, there will be reclosing operation after line trip event. As illustrated in Fig. 4(a), a successful reclosing will trigger frequency spikes in an opposite direction and restoration of the RPAs. In order to avoid duplicated detection and localization caused by the reclosing operation, if two line trip events are detected with opposite frequency spike directions from the same PMUs within a very short period of time, it will be treated as a single line trip event. The RPA before reclosing operations will be utilized to localize this event.

F. Severe Fault Case

In some severe fault cases, such as generation trips and load cutoffs, there would exist frequency deviations in the power grid. As shown in Fig. 4(b) and (c), an example generation trip contains a significant frequency drop while an example load cutoff has a frequency increase in a nine-bus system. In this case, since there is no frequency spike observed, the proposed CCVM-based algorithm can distinguish them from line trip events using the two-times RoCoF check and tuning the threshold T_m given in Fig. 3. Note that if there is a breaker operation right after the generation trip, e.g., operated by the protection, the proposed CCVM-based algorithm would treat it as a line-trip event.

V. Comparison Using Simulation Models

To verify the performance of the proposed algorithm, two IEEE standard power grid models, IEEE 9 and 39 bus systems, are utilized as examples modeled by Power Systems Computer Aided Design (PSCAD). To verify the deployment requirements of different detection methods, the characters and algorithm

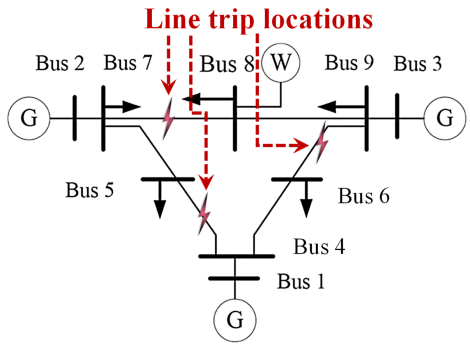

Fig. 5. Illustration of the line trip event locations in IEEE 9 bus system.

capabilities of the model-based and data-based methods are listed in Table II. It concludes that current measurement and the circuit model are necessary for the model-based algorithms. Compared with the methods in [7] and [13], the proposed method can achieve both detection and localization even without the current measurements. Note that the proposed algorithm only uses single phase voltage measurements so that it can be deployed in three phases separately to detect the single-phase trip events.

In this section, the data-based algorithms with voltage measurements are utilized in the comparison considering the PMU deployment cost, where a frequency magnitude (FM)-based detection and localization algorithm [11], [12], as well as a Phase Angle (PA)-based line trip event detection algorithm [10], are also tested. The [13] is not tested since only voltage are available considering the limited installation cost. Currently, the test hardware is based on the Intel Core i7-7700H with 3.6 GHz.

A. IEEE 9 Bus System

The classical IEEE 9 bus system is utilized as an example power grid in this case. Illustrated in Fig. 5, three line trip event locations are tested, i.e., line 4-5, line 6-9, and line 7-8, which are utilized to verify the performance of the proposed algorithms in different locations. The frequency responses, phase angles, and relative phase angles are illustrated in Fig. 6, Fig. 7, and Fig. 8.

By detecting the frequency magnitude values in the frequency peaks, the FM-based algorithm can identify the candidate end buses of the tripped line shown in Fig. 6. In addition, the line

Authorized licensed use limited to: UNIVERSITY OF TENNESSEE LIBRARIES. Downloaded on April 18,2024 at 21:44:51 UTC from IEEE Xplore. Restrictions apply.

TABLE II
DEPLOYMENT REQUIREMENTS FOR ALGORITHMS

Reference	Methodology	Deployment requirements					Capabilities	
		Voltage meas.	Current meas.	System topology	Circuit model	All bus Meas.	Detection	Localization
[4]	Model-based	√	√	√	√	√	√	√
[5]	Model-based	√	√	√	√	√	√	√
[6]	Model-based	√	√	√	√	√	√	√
[7]	Model-based	√	√	√	√	√	√	√
[10]	Data-based	√				√	√	
[11], [12]	Data-based	√		√		√	√	√
[13]	Data-based	√	√	√		√	√	√
Proposed Alg.	Data-based	√		√			√	√

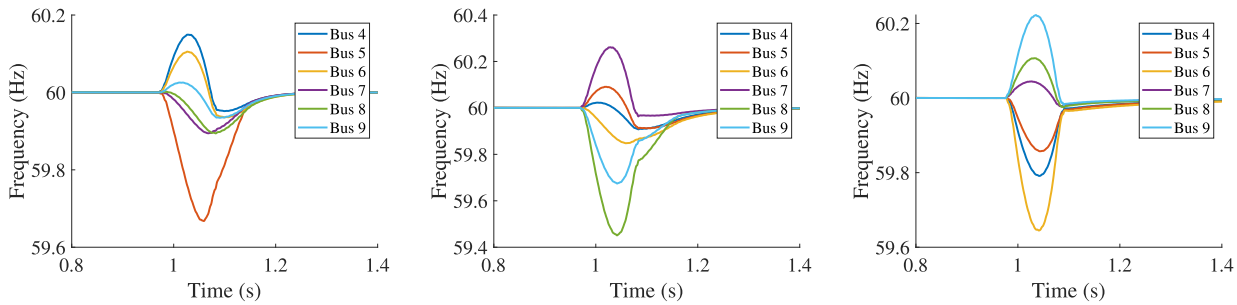

(a) Line trip event between bus 4 and 5 (b) Line trip event between bus 7 and 8 (c) Line trip event between bus 6 and 9

Fig. 6. Frequency simulation results for IEEE 9 bus system.

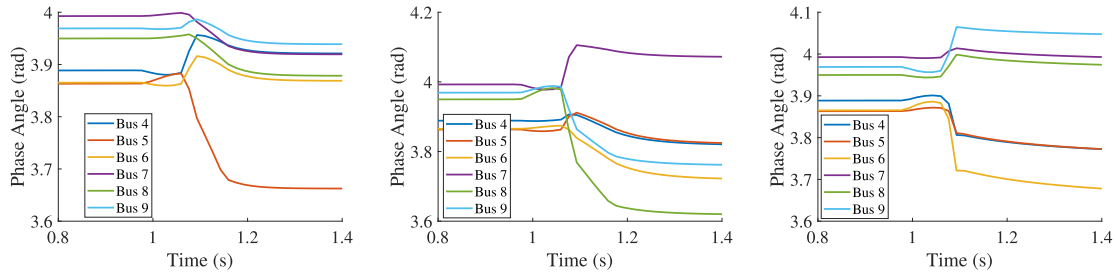

(a) Line trip event between bus 4 and 5 (b) Line trip event between bus 7 and 8 (c) Line trip event between bus 6 and 9

Fig. 7. Phase angle simulation results for IEEE 9 bus system.

trip events can also be detected by checking with the phase angles illustrated in Fig. 7. There are obvious phase angle step changes that indicate there are line trip events by using PA-based algorithms. Alternatively, CCVM-based algorithms can also detect these three line trip events by checking with RoCoFs. The simulation results reveal that FM, PA, and CCVM-based algorithms can successfully detect these three line trip events in the IEEE 9 bus system.

In addition, the line trip event localization results from the FM-based algorithm are obvious that the largest and the smallest frequency spikes in Fig. 6 are exactly the end buses of the tripped lines. Additionally, the largest and smallest relative phase angles are shown in Fig. 8. And it provides similar results by using RPA-based algorithm. This verifies that both FM and RPA-based algorithms can successfully identify the line trip event in the IEEE 9 bus system. Note that the reference buses are bus 9 in the first two cases and bus 4 in the last case. However, the PA-based algorithm is not able to identify the line trip event locations by using the phase angle measurements.

B. IEEE 39 Bus System

To further verify the performance under a complicated topology, IEEE 39 bus system is utilized in this case where the line trip event locations are line 1-2, line 10-11, and line 23-24, as demonstrated in Fig. 9. A line trip event detection and localization accuracy comparison among FM-based, PA-based, and proposed algorithms with both IEEE 9 and 39 bus systems are summarized in Table III. The value of localization accuracy for FM-based is NaN because it does not have localization ability. For the speed of different methods, a line trip event can be detected in 2.07 ms for the proposed method and it is treated as the benchmark. The PA-based method would consume 6.03 times the time with 10-point data even under 8 parallel computing units according to [10]. It can be revealed that the accuracy of the PA-based method under the IEEE 39 bus is 20.6% lower than the proposed method. The reason is that this method can not handle the cases that the power flow direction change is caused by the line trip events.

Authorized licensed use limited to: UNIVERSITY OF TENNESSEE LIBRARIES. Downloaded on April 18,2024 at 21:44:51 UTC from IEEE Xplore. Restrictions apply.

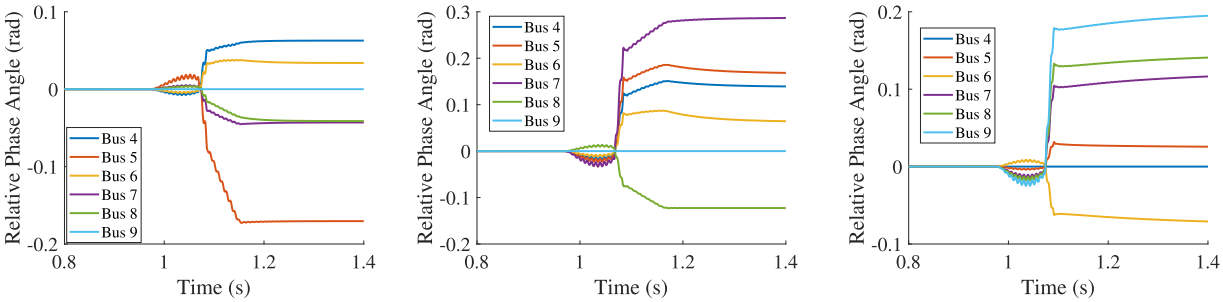

(a) Line trip event between bus 4 and 5 (b) Line trip event between bus 7 and 8 (c) Line trip event between bus 6 and 9

Fig. 8. Relative phase angle simulation results for IEEE 9 bus system.

TABLE III
LINE TRIP EVENT DETECTION AND LOCALIZATION COMPARISON

Algorithms	Detection accuracy		Localization accuracy		Average accuracy	Computational complexity	Speed: Benchmark is 2.07 ms
	IEEE 9 . bus sys.	IEEE 39 bus sys.	IEEE 9 bus sys.	IEEE 39 bus sys.			
PA-based alg. [10]	100%	100%	NaN	NaN	100%	O(n^3)	6.03
FM-based alg. [12]	100%	100%	100%	79.4%	94.85%	O(n)	0.56
CCVM-RPA	100%	100%	100%	100%	100%	O($nlog(n)$)	1.00

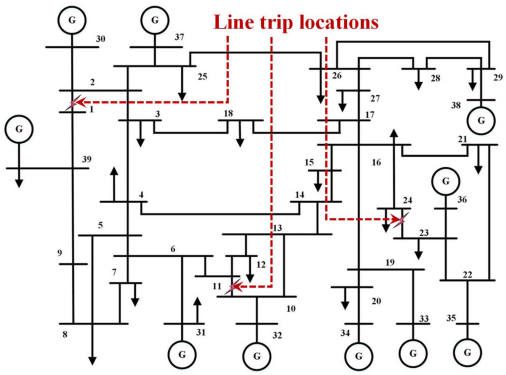

Fig. 9. Illustration of the line trip event locations in IEEE 39 bus system.

Compared with the FM-based algorithm, the proposed algorithm has 1.26 times (100/79.4) higher accuracy on the line trip event localization dealing with high impedance cases. In addition, the line trip event detection for all algorithms is very accurate. The comparison of computational complexity indicates that the FM-based algorithm can achieve a very quick calculation and the PA-based algorithm needs to consume more computing resources. To speed up the computation, the operations of the proposed algorithm can be highly parallelizable to process the data from multiple PMUs. Two special cases are discussed in the following sub-sections.

1) Power Flow Direction Change Case: Again, the frequency of responses during the event is given in Fig. 10. Two power flow direction change cases in lines 1-2 and lines 23-24 indicate that the frequency magnitude change for all buses are in the same direction so it would be not possible to identify the line trip event locations with FM-based algorithms. This is because the power flow direction on bus 1 and bus 24 changed after the line trip event so that the frequency change directions for all buses keep the same while relative phase angle oscillations are observed on bus 1 and bus 24. In contrast, with RPA-based algorithm, the tripped lines are still successfully localized where the largest and smallest relative phase angles for all three cases are illustrated in Fig. 11. These kinds of special cases have caused the relatively low accuracy of FM-based algorithm as listed in Table III.

TABLE IV
CANDIDATE TRIPPED LINES WITH A LIMITED NUMBER OF SENSORS

Cases	Line 1-2	Line 10-11	Line 23-24
Candidate Lines	**1-2**, 2-3, 2-25	5-6, 6-7, 6-11	16-21, 16-24, 21-22
	2-30	**10-11**, 11-12	22-23, **23-24**, 23-36

2) Limited Number of Sensor Case: In this case, only one-third of buses (13 buses, e.g., No.1,4,7...,37) in the IEEE 39 bus system have PMUs deployed. Similarly, three line trip event locations, i.e., line 1-2, line 10-11, and line 23-24, are tested with a limited number of PMUs. The candidate bus results are summarized in Table IV. All three tripped lines (bold font) are found in the candidate line list under three test cases. This result verifies the profound performance of the proposed RPA and TR-based algorithms under a limited number of sensor cases.

VI. EXPERIMENT RESULTS FOR WIDE-AREA CASE

To further verify the real-world performance of the proposed algorithm, the wide-area based experiments are conducted using the field measurements. Frequency measurements recorded by FNET/GridEye are utilized to detect line trip events from EI and WECC where more than 200 PMUs have been deployed in

Authorized licensed use limited to: UNIVERSITY OF TENNESSEE LIBRARIES. Downloaded on April 18,2024 at 21:44:51 UTC from IEEE Xplore. Restrictions apply.

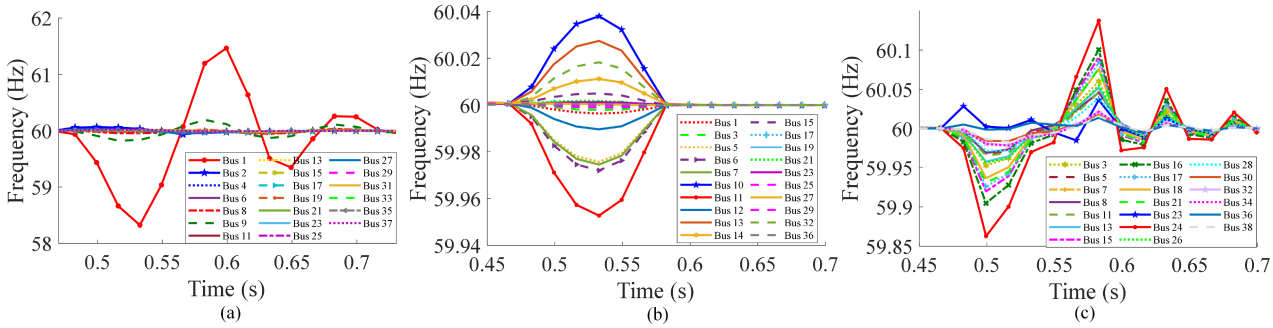

Fig. 10. Frequency simulation results for IEEE 39 bus system. (a) Line trip event between bus 1 and 2. (b) Line trip event between bus 10 and 11. (c) Line trip event between bus 23 and 24.

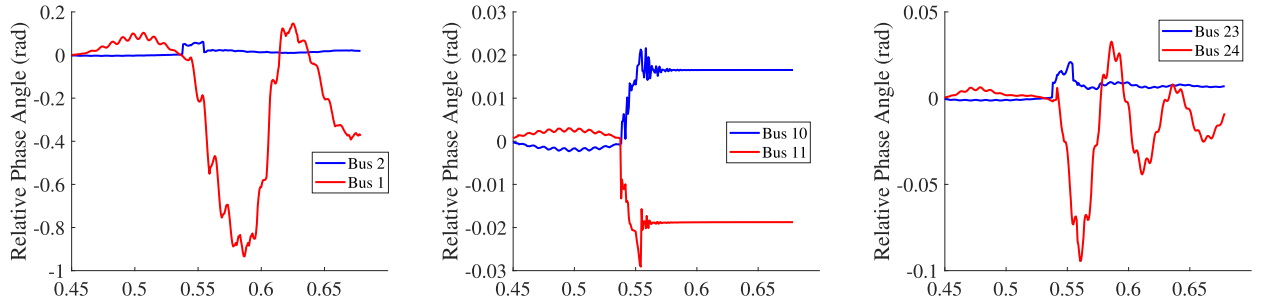

(a) Line trip event between bus 1 and 2 (b) Line trip event between bus 10 and 11 (c) Line trip event between bus 23 and 24

Fig. 11. Candidate tripped line estimated from relative phase angle for IEEE 39 bus system.

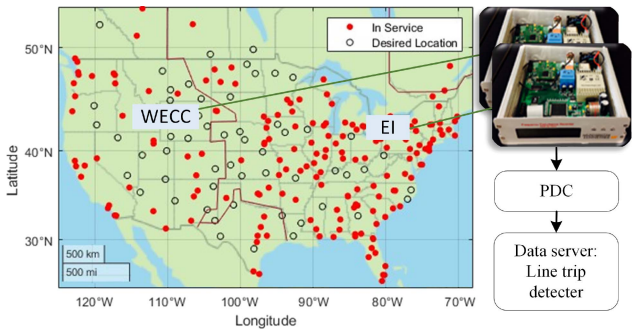

Fig. 12. Location of the FDRs in FNET/GridEye.

the U.S. for national scale wide-area monitoring purposes, as shown in Fig. 12. The frequency estimation algorithm deployed in the FNET is using DFT-based algorithm with 6 cycle window and 10 Hz reporting rate [37] which satisfies the requirements in (10). However, as a result of the long DFT window, RoCoF values are relatively lower than those in the simulation results.

A. EI Case Study

The first case is a line trip event captured in EI on Feb. 6th, 2020. An event data summary is listed in Table V. The total event recording time is 40 s while GPS positioning information, the longitude, and latitude, are utilized for event localization. In this line trip event, totally of 56 PMUs have detected this event by using the CCVM-based algorithm, as illustrated in Fig. 13.

TABLE V
EVENT DATA SUMMARY

Interconnection	Involved PMUs	Recorded time	Event time
EI	56	40s	2020-02-06 19.10.41
WECC	17	40s	2020-02-03 04.29.04

By deploying RPA-based algorithm, 48 PMUs are categorized into the VPSG (marked in blue stars) and 7 PMUs are categorized into the VPRG (marked in red stars). By visualizing the mean frequency responses in both the VPSG and VPRG, it would be challenging to identify the mean frequency responses that have frequency spikes in two opposite directions. However, by checking with the RPAs, the i_a and i_b can be clearly identified as shown in the RPA response in Fig. 13. This verifies the benefit of RPA-based algorithm toward FM-based algorithm in the wide-area power system.

Since the real-time power grids topology information is unavailable for wide-area power grid including many utility entities, the i_a and i_b are directly identified by using RPA-based algorithm and marked in black squares. Since i_a and i_b are located on the boundary of VPSG and VPRG, the tripped line should be located between them. However, due to lacking more

Authorized licensed use limited to: UNIVERSITY OF TENNESSEE LIBRARIES. Downloaded on April 18,2024 at 21:44:51 UTC from IEEE Xplore. Restrictions apply.

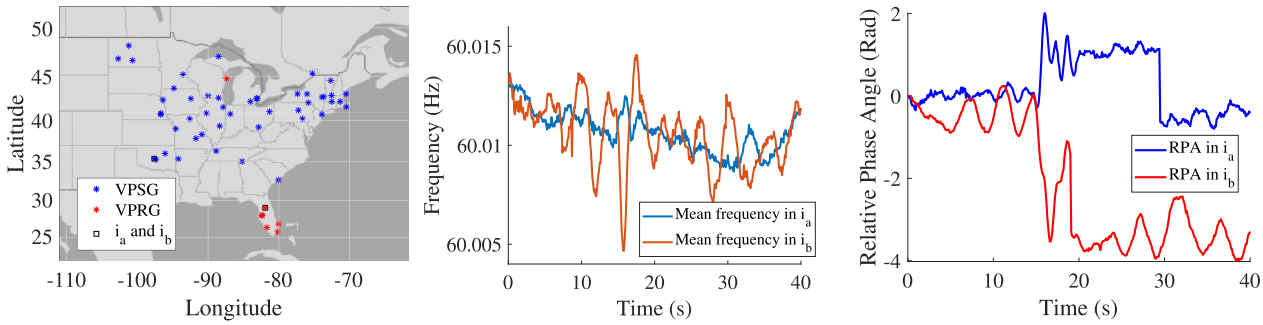

(a) FDR deployment map in EI (b) Mean frequency responses (c) RPA responses

Fig. 13. Experiment test results in EI recorded on Feb. 6th, 2020.

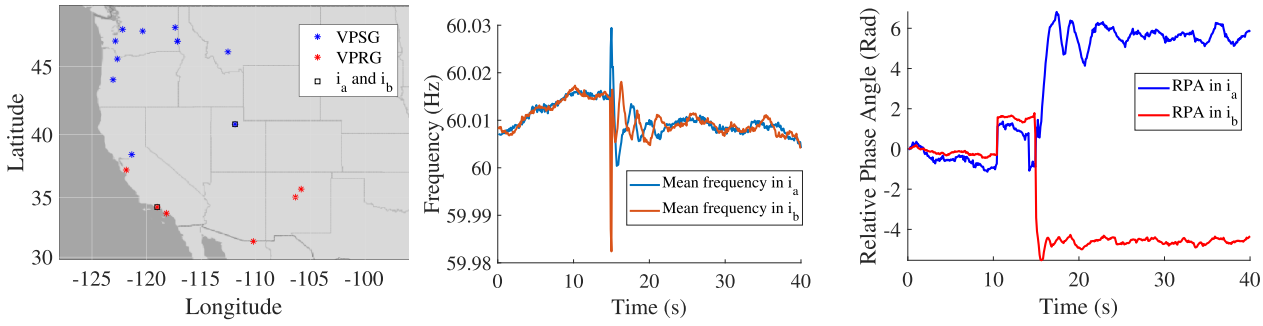

(a) FDR deployment map in WECC (b) Mean frequency responses (c) RPA responses

Fig. 14. Experiment test results in WECC recorded Feb. 3 rd, 2020.

PMUs and power grid topology information, the conclusion for the line trip event localization is that one or multiple lines between i_a and i_b can be the tripped lines. This verifies the benefit of RPA-based algorithm that the line trip event can be roughly localized even though the power grid topology is not available in wide-area cases.

B. WECC Case Study

The second case is a line trip event captured on Feb. 3 rd, 2020 in the WECC. The event information is also listed in Table V, where 17 PMUs have detected this event by using CCVM-based algorithm. As can be seen in Fig. 14, 11 PMUs are categorized into the VPSG while 6 PMUs are categorized into the VPRG. PMUs with the same color indicate that the average frequency and the largest RPA responses from the two categories provide the same trend as the previous case did. It is interesting to notice that the frequency spikes, in this case, are obvious compared with the previous case and the RPA step change is also larger.

In this case, both FM and RPA-based algorithms can localize the line trip event easily. The potential reason is that the PMUs deployment locations may be closer to the line trip event location so that the RoCoF values are larger and the frequency spikes are obvious enough to be captured. The i_a and i_b are marked in the black squares which give the virtual power flow directions and the candidate line trip event locations. However, because the number of PMU is limited to accurately localize the event, only a rough event location between i_a and i_b is estimated.

VII. Conclusion

To accurately detect and locate the line trip events, this article proposes a real-time CCVM-based line trip event detection algorithm and a RPA-based line trip event localization algorithm, respectively. The CCVM-based algorithm is discussed in terms of frequency estimation, RoCoF calculation, and detection algorithm aspects. Then, the RPA-based algorithm is presented with the analysis under two standard circuit cases. Based on the TR-based algorithm, the limited number of sensor case demonstrates that all the tripped lines are successfully detected. In the simulation test cases, the performance of the proposed CCVM and RPA-based algorithms are verified by comparing with a PA-based algorithm and a FM-based algorithm. The line trip event can be detected in 2.07 ms and a 1.26 time accuracy improvement can be observed compared with the FM-based one. Moreover, in the actual experiment, two actual cases collected from EI and WECC are presented to verify the online performance of the proposed algorithms in wide-area power systems.

References

[1] A. Qiu, A. W. Al-Dabbagh, and T. Chen, "A tradeoff approach for optimal event-triggered fault detection," *IEEE Trans. Ind. Electron.*, vol. 66, no. 3, pp. 2111–2121, Mar. 2019.

Authorized licensed use limited to: UNIVERSITY OF TENNESSEE LIBRARIES. Downloaded on April 18,2024 at 21:44:51 UTC from IEEE Xplore. Restrictions apply.

[2] M. Mditshwa, M. E. S. Mnguni, and M. Ratshitanga, "A review on sustaining power system frequency stability considering the integration of distributed energy resources (DERs)," in *Proc. IEEE 30th Southern Afr. Universities Power Eng. Conf.*, 2022, pp. 1–6.
[3] M. Amyotte and M. Ordonez, "Power loss prediction for distributed energy resources: Rapid loss estimation equation," *IEEE Trans. Ind. Electron.*, vol. 68, no. 3, pp. 2289–2299, Mar. 2021.
[4] X. Yang, N. Chen, and C. Zhai, "A control chart approach to power system line outage detection under transient dynamics," *IEEE Trans. Power Syst.*, vol. 36, no. 1, pp. 127–135, Jan. 2021.
[5] M. Ghofrani, S. Talaei, P. Nguyen, A. Suherli, and A. Arabali, "A novel AC model for multiple-line outage detection," in *Proc. IEEE Power Energy Conf. Illinois*, 2017, pp. 1–6.
[6] S. Nie, L. Ding, and W. Li, "Multiple line-outage detection in power system with load stochastic perturbations," *IEEE Trans. Circuits Syst. II: Exp. Briefs*, vol. 67, no. 10, pp. 1994–1998, Oct. 2020.
[7] A. Dwivedi and A. Tajer, "Scalable quickest line outage detection and localization via graph spectral analysis," *IEEE Trans. Power Syst.*, vol. 37, no. 1, pp. 590–602, Jan. 2022.
[8] X. Liu, J. Du, and Z. -S. Ye, "A condition monitoring and fault isolation system for wind turbine based on SCADA data," *IEEE Trans. Ind. Inform.*, vol. 18, no. 2, pp. 986–995, Feb. 2022.
[9] L. G. Meegahapola, S. Bu, D. P. Wadduwage, C. Y. Chung, and X. Yu, "Review on oscillatory stability in power grids with renewable energy sources: Monitoring, analysis, and control using synchrophasor technology," *IEEE Trans. Ind. Electron.*, vol. 68, no. 1, pp. 519–531, Jan. 2021.
[10] J. E. Tate and T. J. Overbye, "Line outage detection using phasor angle measurements," *IEEE Trans. Power Syst.*, vol. 23, no. 4, pp. 1644–1652, Nov. 2008.
[11] G. Rovatsos, X. Jiang, A. D. Domínguez-Garcia, and V. V. Veeravalli, "Statistical power system line outage detection under transient dynamics," *IEEE Trans. Signal Process.*, vol. 65, no. 11, pp. 2787–2797, Jun. 2017.
[12] D. Zhou, Y. Liu, and J. Dong, "Frequency-based real-time line trip detection and alarm trigger development," in *Proc. IEEE PES Gen. Meeting Conf. Expo.*, 2014, pp. 1–5.
[13] X. Deng, D. Bian, D. Shi, W. Yao, Z. Jiang, and Y. Liu, "Line outage detection and localization via synchrophasor measurement," in *Proc. IEEE Innov. Smart Grid Technol. - Asia*, 2019, pp. 3373–3378.
[14] D. Carrión, J. W. González, I. A. Issac, and G. J. López, "Optimal fault location in transmission lines using hybrid method," in *Proc. IEEE PES Innov. Smart Grid Technol. Conf. - Latin Amer.*, 2017, pp. 1–6.
[15] Y. Zhou, R. Arghandeh, H. Zou, and C. J. Spanos, "Nonparametric event detection in multiple time series for power distribution networks," *IEEE Trans. Ind. Electron.*, vol. 66, no. 2, pp. 1619–1628, Feb. 2019.
[16] G. Zheng, Y. Liu, and G. Radman, "Wide area frequency based generation trip event location estimation," in *Proc. IEEE Power Energy Soc. Gen. Meeting*, 2012, pp. 1–6.
[17] B. Wang, Y. Liu, D. Lu, K. Yue, and R. Fan, "Transmission line fault location in MMC-HVDC grids based on dynamic state estimation and gradient descent," *IEEE Trans. Power Del.*, vol. 36, no. 3, pp. 1714–1725, Jun. 2021.
[18] S. Zhang, Y. Wang, M. Liu, and Z. Bao, "Data-based line trip fault prediction in power systems using LSTM networks and SVM," *IEEE Access*, vol. 6, pp. 7675–7686, 2018.
[19] G. Zheng, G. Radman, W. Guan, and S. Yang, "Wide area phasor measurements based disturbance monitoring for line trip event," in *Proc. IEEE Power Energy Soc. Gen. Meeting*, 2013, pp. 1–5.
[20] L. Guo, R. Li, and B. Jiang, "A data-driven long time-series electrical line trip fault prediction method using an improved stacked-informer network," *Sensors*, vol. 21, no. 13, 2021, Art. no. 4466.
[21] T. Lan, Y. Lin, J. Wang, B. Leao, and D. Fradkin, "Unsupervised power system event detection and classification using unlabeled PMU data," in *Proc. IEEE PES Innov. Smart Grid Technol. Europe*, 2021, pp. 01–05.
[22] N. Ehsani, F. Aminifar, and H. Mohsenian-Rad, "Convolutional autoencoder anomaly detection and classification based on distribution PMU measurements," *IET Gener., Transmiss. Distrib.*, vol. 16, no. 14, pp. 2816–2828, 2022.
[23] M. Cui, J. Wang, J. Tan, A. R. Florita, and Y. Zhang, "A novel event detection method using PMU data with high precision," *IEEE Trans. Power Syst.*, vol. 34, no. 1, pp. 454–466, Jan. 2019.
[24] Y. Liu et al., "Recent developments of FNET/GridEye–A situational awareness tool for smart grid," *CSEE J. Power Energy Syst.*, vol. 2, no. 3, pp. 19–27, Sep. 2016.
[25] S. Liu et al., "Practical event location estimation algorithm for power transmission system based on triangulation and oscillation intensity," *IEEE Trans. Power Del.*, vol. 37, no. 6, pp. 5190–5202, Dec. 2022.
[26] PSCAD, "IEEE 9 bus system," 2018. [Online]. Available: https://www.pscad.com/knowledge-base/download/ieee_9_bus_technical_note.pdf
[27] S. Som, R. Dutta, A. Gholami, A.K. Srivastava, S. Chakrabarti, and S. R. Sahoo, "DPMU-based multiple event detection in a microgrid considering measurement anomalies," *Appl. Energy*, vol. 308, 2022, Art. no. 118269.
[28] J. Zhao, L. Zhan, H. Yin, F. Li, W. Yao, and Y. Liu, "Recent development of frequency estimation methods for future smart grid," *IEEE Open Access J. Power Energy*, vol. 7, pp. 354–365, 2020.
[29] Z. Ali, N. Christofides, L. Hadjidemetriou, E. Kyriakides, Y. Yang, and F. Blaabjerg, "Three-phase phase-locked loop synchronization algorithms for grid-connected renewable energy systems: A review," *Renewable Sustain. Energy Rev.*, vol. 90, pp. 434–452, 2018.
[30] A. Carboni and A. Ferrero, "A Fourier transform-based frequency estimation algorithm," *IEEE Trans. Instrum. Meas.*, vol. 67, no. 7, pp. 1722–1728, Jul. 2018.
[31] *IEEE Standard for Synchrophasor Measurements for Power Systems*, IEEE Standard C37.118.1-2011 (Revision of IEEE Standard C37.118-2005), 2011.
[32] H. Yin et al., "Precise RoCoF estimation algorithm for low inertia power grids," *Electric Power Syst. Res.*, vol. 209, 2022, Art. no. 107968.
[33] S. You et al., "Calculate center-of-inertia frequency and system RoCoF using PMU data," in *Proc. IEEE Power Energy Soc. Gen. Meeting*, 2021, pp. 1–5.
[34] P. Shaw and M. K. Jena, "A novel event detection and classification scheme using wide-area frequency measurements," *IEEE Trans. Smart Grid*, vol. 12, no. 3, pp. 2320–2330, May 2021.
[35] D. Deka, M. Chertkov, and S. Backhaus, "Topology estimation using graphical models in multi-phase power distribution grids," *IEEE Trans. Power Syst.*, vol. 35, no. 3, pp. 1663–1673, May 2020.
[36] J. Guo et al., "Design and implementation of a real-time off-grid operation detection tool from a wide-area measurements perspective," *IEEE Trans. Smart Grid*, vol. 6, no. 4, pp. 2080–2087, Jul. 2015.
[37] L. Zhan, J. Zhao, J. Culliss, Y. Liu, Y. Liu, and S. Gao, "Universal grid analyzer design and development," in *Proc. IEEE Power Energy Soc. Gen. Meeting*, 2015, pp. 1–5.

He Yin (Senior Member, IEEE) received the B.S. degree in electrical and computer engineering from the University of Michigan-Shanghai Jiao Tong University Joint Institute, Shanghai, China, in 2012, and the Ph.D. degree from Shanghai Jiao Tong University, Shanghai, China, in 2017. He is currently a Research Assistant Professor with the Center for Ultra-Wide-Area Resilient Electric Energy Transmission Networks, University of Tennessee, Knoxville, TN, USA. His research interests include situational awareness, renewable energy source control, optimization, decentralized control of microgird, and PMU design.

Wei Qiu (Member, IEEE) received the B.Sc. degree in electrical engineering from the Hubei University of Technology, Wuhan, China, in 2015, and the M.Sc. and Ph.D. degrees in electrical engineering from Hunan University, Changsha, China, in 2017 and 2021, respectively. From 2019 to 2021, he was a Joint Doctoral Student at the University of Tennessee, Knoxville, TN, USA. He is currently a Research Associate with the Department of Electrical Engineering and Computer Science, University of Tennessee. His research interests include situational awareness, cyber-security of synchrophasor, and power quality measurement.

Authorized licensed use limited to: UNIVERSITY OF TENNESSEE LIBRARIES. Downloaded on April 18,2024 at 21:44:51 UTC from IEEE Xplore. Restrictions apply.

Yuru Wu (Student Member, IEEE) received the B.S.E. degree in electronic engineering from the Tsinghua University, Beijing, China, in 2017. He is currently working toward the Ph.D. degree in power electronic engineering with the University of Tennessee, Knoxville, TN, USA. His research interests include phase measurement unit design, power quality in grid, noise analysis, and algorithm design.

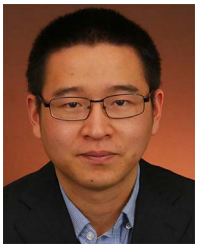

Shutang You (Senior Member, IEEE) received the B.S. and M.S. degrees in electrical engineering from Xi'an Jiaotong University, Xi'an, China, in 2011 and 2014, respectively, and the Ph.D. degree in electrical engineering from the University of Tennessee, Knoxville, TN, USA, in 2017. From 2018 to 2021, he was a Research Assistant Professor at the Department of Electrical Engineering and Computer Science. He is currently an Engineer with EDP renewables, Madrid, NM, USA. His research interests include power grid dynamics and monitoring.

Yuqing Dong (Member, IEEE) received the B.S. and Ph.D. degrees from the College of Electrical Engineering, Sichuan University, Chengdu, China, in 2017 and 2022, respectively. From 2019 to 2021, she was a Joint Doctoral Student at the University of Tennessee, Knoxville, TN, USA. She is currently a Research Associate with the Department of Electrical Engineering and Computer Science, University of Tennessee. Her research interests include high voltage direct current and power system stability.

Wenpeng Yu (Member, IEEE) received the Ph.D. degrees in electrical engineering from the Shanghai Jiaotong University, Shanghai, China, in 2014. He is currently a Research Assistant Professor with the Department of Electrical Engineering and Computer Science, University of Tennessee, Knoxville, TN, USA. His research interests include power system analysis, event and oscillation detection and analysis, synchrophasor measurement based analysis, and active distribution networks.

Yilu Liu (Fellow, IEEE) received the B.S. degree from Xi'an Jiaotong University, Xi'an, China, and the M.S. and Ph.D. degrees from Ohio State University, Columbus, OH, USA, in 1986 and 1989, respectively. She is currently the Governor's Chair of the University of Tennessee, Knoxville (UTK), TN, USA, and Oak Ridge National Laboratory (ORNL), Oak Ridge, TN. She is also the Deputy Director of the DOE/NSF-cofunded Engineering Research Center CURENT, prior to joining UTK/ORNL and a Professor with Virginia Tech. She led the effort to create the North American power grid Frequency Monitoring Network (FNET) at Virginia Tech, which is now operated at UTK and ORNL as GridEye. Her current research interests include power system wide-area monitoring and control, large interconnection-level dynamic simulations, electromagnetic transient analysis, and power transformer modeling and diagnosis. In 2016, she was elected as the Member of the National Academy of Engineering.

Authorized licensed use limited to: UNIVERSITY OF TENNESSEE LIBRARIES. Downloaded on April 18,2024 at 21:44:51 UTC from IEEE Xplore. Restrictions apply.